THE JOURNAL OF BIOLOGICAL CHEMISTRY VOL. 284, NO. 48, pp. 33614–33622, November 27, 2009

The *Arabidopsis* ATP-binding Cassette Protein AtMRP5/AtABCC5 Is a High Affinity Inositol Hexa*kis*phosphate Transporter Involved in Guard Cell Signaling and Phytate Storage*[S]

Received for publication, June 5, 2009, and in revised form, September 17, 2009 Published, JBC Papers in Press, September 21, 2009, DOI 10.1074/jbc.M109.030247

Réka Nagy[‡1], Hanne Grob[‡], Barbara Weder[‡], Porntip Green[§], Markus Klein[¶], Annie Frelet-Barrand[‡], Jan K. Schjoerring[‖], Charles Brearley[§2], and Enrico Martinoia[‡]**

*From the [‡]University of Zurich, Institute of Plant Biology, Zollikerstrasse 107, CH-8008 Zürich, Switzerland, **POSTECH-UZH Global Research Laboratory, Division of Molecular Life Sciences, Pohang University of Science and Technology, Pohang 790-784, Korea, [¶]Tobacco Technologies, Tobacco Applied Biology, Philip Morris International, R & D Innnovation Cube, Quai Jeanrenaud 5, CH-2000 Neuchatel, Switzerland, the [‖]University of Copenhagen, Faculty of Life Sciences, Thorvaldsensvej 40, DK-1871 Frederiksberg C, Denmark, and the [§]University of East Anglia, School of Biological Sciences, Norfolk NR4 7TJ, Norwich, United Kingdom*

Arabidopsis* possesses a superfamily of ATP-binding cassette (ABC) transporters. Among these, the multidrug resistance-associated protein AtMRP5/AtABCC5 regulates stomatal aperture and controls plasma membrane anion channels of guard cells. Remarkably, despite the prominent role of AtMRP5 in conferring partial drought insensitivity upon *Arabidopsis*, we know little of the biochemical function of AtMRP5. Our phylogenetic analysis showed that AtMRP5 is closely related to maize MRP4, mutation of which confers a low inositol hexa*kis*phosphate kernel phenotype. We now show that insertion mutants of *AtMRP5* display a low inositol hexa*kis*phosphate phenotype in seed tissue and that this phenotype is associated with alterations of mineral cation and phosphate status. By heterologous expression in yeast, we demonstrate that AtMRP5 encodes a specific and high affinity ATP-dependent inositol hexa*kis*phosphate transporter that is sensitive to inhibitors of ABC transporters. Moreover, complementation of the *mrp5-1* insertion mutants of *Arabidopsis* with the AtMRP5 cDNA driven from a guard cell-specific promoter restores the sensitivity of the mutant to abscisic acid-mediated inhibition of stomatal opening. Additionally, we show that mutation of residues of the Walker B motif prevents restoring the multiple phenotypes associated with *mrp5-1*. Our findings highlight a novel function of plant ABC transporters that may be relevant to other kingdoms. They also extend the signaling repertoire of this ubiquitous inositol polyphosphate signaling molecule.

Guard cells form pairs of cells, which are conjoined at their ends, in the epidermis of the aerial tissues of plants. The cells surround a central pore, the stoma, through which gas exchange occurs. The principal gases exchanged are CO_2 and water vapor, and the function of the stomatal complex may be considered as the maximization of CO_2 assimilation by photosynthesis for the minimization of water loss.

Guard cells and hence the aperture of the central pore are sensitive to environmental factors including light, temperature, CO_2, and ozone (1). Stomatal closure is initiated by the drought stress hormone abscisic acid (ABA).[3] The closure of stomata is a result of a loss of turgor of the delimiting guard cells as a consequence of ion efflux, predominantly Cl^- and K^+, and metabolic conversion of organic acids into starch (2).

Although the molecular identity of genes encoding the outward and inward K^+ conductances are known for *Arabidopsis thaliana* (3), it remains to be demonstrated whether the recently identified SLAC protein (4, 5) encodes the S-type anion channel or is a subunit thereof.

The ATP-binding cassette family of membrane proteins is among the most ubiquitous and variable group of membrane proteins and is most commonly associated with membrane transport phenomena. The substrates transported are especially diverse, and consequently a major obstacle to the interpretation of ABC transporter function, particularly pertinent in the context of guard cell function, is the identification of the substrate transported.

A recent study identified the ABC transporter AtABCB14 as an apoplast to symplast malate importer capable of modulating stomatal response to CO_2 (6), whereas plants bearing mutations in the MRP type ABC transporter *AtMRP5* show partial inhibition of ABA-induced stomatal closure (7); impairment of activation of S-type anion channels by both ABA and cytosolic Ca^{2+} (8); and, additionally, impairment of the activation of plasma membrane Ca^{2+}-permeable channel activity by ABA (8). A number of hypotheses have been proposed to explain the phenotype of *atmrp5* mutants; these hypotheses include that *AtMRP5* encodes an anion channel or that AtMRP5 directly regulates a guard cell anion channel (8). Both of these possibil-

* This work was funded by Swiss National Foundation Grant 3100AO-117790 (to E. M.), by funds from the Forschungskredit der Universität Zürich (to R. N.), by European Union Project Public Health Impact on Long Term, Low Level Mixed Element Exposure (PHIME) Contract FOOD-CT-2006-0016253 (to J. K. S.), and by Biotechnology and Biological Sciences Research Council Grant BB/C514090/1 (to C. B.).

[S] The on-line version of this article (available at http://www.jbc.org) contains supplemental text and Figs. S1–S6.

[1] To whom correspondence may be addressed. Tel.: 41-44-6348283; Fax: 41-44-6348204; E-mail: rnagy@botinst.uzh.ch.

[2] To whom correspondence may be addressed. Tel.: 44-1603592197; Fax: 44-1603592250; E-mail: C.Brearley@uea.ac.uk.

[3] The abbreviations used are: ABA, abscisic acid; ABC, ATP-binding cassette; HPLC, high pressure liquid chromatography; AMPPNP, adenyl-5′-yl imidodiphosphate; MES, 4-morpholineethanesulfonic acid; insP_6 inositol hexa*kis*phosphate.

ities have precedent in the cystic fibrosis transmembrane conductance regulator, a mammalian ABC protein that has ion (Cl^-) channel activity and that also modulates the activity of associated ion channels (9).

The activity of other Cl^- conductances, but not cystic fibrosis transmembrane conductance regulator, have been shown to be influenced by inositol polyphosphate signaling molecules (10, 11). Most recently, inositol 3,4,5,6-tetra*kis*phosphate was identified as a physiological regulator of a specific chloride conductance, that of the CIC-3 channel of mammalian secretory epithelia (12).

Inositol 3,4,5,6-tetra*kis*phosphate and inositol 1,4,5-trisphosphate are not the only inositol phosphates that directly regulate ion channels. In guard cells, inositol hexa*kis*phosphate mobilizes calcium from endomembrane stores (13) and inhibits the inward rectifying K^+ conductance (14).

We were fascinated by a recent report that disruption of a gene encoding the ATP-binding cassette protein *ZmMRP4* reduced inositol hexa*kis*phosphate accumulation in maize kernels (15). One interpretation of this report is that ZmMRP4 is responsible for transport of inositol hexa*kis*phosphate or a precursor across the vacuole membrane of inositol hexa*kis*phosphate storage tissues of maize kernels.

Our experiments have addressed the function of AtMRP5, an orthologue of ZmMRP4, *in planta*. By a combination of biochemical, physiological, and genetic analysis, we identify a hitherto undescribed inositol polyphosphate transport function in *Arabidopsis* for this example of the most ubiquitous class of membrane transport proteins. Our work links inositol hexa*kis*phosphate transport to the regulation of stomatal response to ABA.

EXPERIMENTAL PROCEDURES

Chemical Analysis of AtMRP5 Loss-of-function Mutants—Fifty milligrams of dried seed material was incinerated for 8 h at 550 °C, and subsequently the ash was solubilized in 2 ml of 6 N HCl, briefly heated up to 100 °C, purified through Whatman No. 40 ashless filter paper, and transferred to double-distilled water to a total volume of 50 ml. Element contents were measured by inductively coupled plasma emission-spectroscopy analysis with a Varian Liberty 220 (Varian Inc., Palo Alto, CA) equipped with an ultrasonic nebulizer (CETAC U-5000 AT^+) according to standard procedures. Inositol hexa*kis*phosphate and inorganic phosphate were determined by suppressed ion conductivity HPLC of acid extracts of *Arabidopsis* seeds (16). Seeds, 2–4 mg, were boiled in 0.8 ml of 0.6 M-HCl for 30 min, and the supernatant was diluted 10 times in water. The samples (50 μl) were analyzed on a Dionex ICS2000 chromatography system fitted with a 25-cm × 2-mm internal diameter Dionex AS11 anion exchange column, with an associated AG11 guard column. The column was eluted with a gradient of KOH (0 min, 0 mM KOH; 20 min, 100 mM KOH) at a flow rate of 0.25 ml/min. The inositol hexa*kis*phosphate and P_i content of samples was determined from a calibration curve of peak area *versus* the amount injected in the range 0.2–4 and 0.2–2 nmol, respectively. In our hands, leaf inositol hexa*kis*phosphate levels were below the limit of detection of this method.

Functional Analysis in Yeast—The *ycf1* yeast mutant was transformed with the expression vector pNEV harboring no insert (pNEV) or *AtMRP5* cDNA (pNEV-MRP5). Microsomal vesicles were isolated as described previously (17). For the transport of inositol hexa*kis*phosphate, Ins(1,[^{33}P]2,3,4,5,6)P_6 prepared according to (18) was added to the reaction mix consisting of transport buffer, 1 mM dithiothreitol, 5 mM ATP, 10 mM $MgCl_2$, 10 mM creatine phosphate, and 100 μg/ml creatine kinase. Yeast microsomes were added to start the transport assay. The assays were performed at room temperature. At intervals, inositol hexa*kis*phosphate uptake was terminated by the transfer of three aliquots, equivalent to 18.9 nCi (700 Bq) of starting material, onto 0.45-μm-diameter pore size nitrocellulose filters. Under these conditions, the rate of net transport was linear with time during the first 5.5 min. The values are corrected for corresponding controls with vesicles isolated from *ycf1* yeasts transformed with the empty pNEV vector. ATP-independent inositol hexa*kis*phosphate uptake was assessed in the absence of ATP. Transport assays for all treatments were performed with the same vesicle preparation. The experiments were repeated three times, with independent vesicle preparations. Labeled material recovered on the filter was analyzed by Partisphere SAX HPLC. For the experiments with the nonhydrolyzable ATP analogue AMPPNP, the 4 mM ATP from the reaction mix was replaced with the equivalent concentration of AMPPNP. For the experiments on ice, the tubes containing the reaction mix and the labeled $InsP_6$ were placed on ice immediately after the addition of the yeast microsomes.

Inhibition Studies—Yeast microsomes were incubated at room temperature in the reaction mix that contained the indicated potential inhibitors (see Table 1). After 8 min, Ins(1,[^{33}P]2,3,4,5,6)P_6 was added to the reaction mix, and inositol hexa*kis*phosphate uptake was determined as above. The different inhibitors were always tested with the same vesicle preparation as the Ins(1,[^{33}P]2,3,4,5,6)P_6 uptake control. The number of repetitions is indicated in Table 1. For experiments with different inositol polyphosphates (see Table 2), the putative inhibitors/competitors were added to the reaction mix at the concentration indicated in Table 2. The transport assay was started by the addition of microsomes. The assays were performed at room temperature. After 5.5 min, uptake was terminated by the transfer of three replicates onto 0.45-μm-diameter pore size nitrocellulose filters. The number of repetitions of the experiment is indicated in Table 2. ATP-dependent AtMRP5-mediated transport was considered as 100%. The reaction mix contained labeled $InsP_6$ at 1.85 kBq/nitrocellulose filter.

Partisphere SAX HPLC—Extracts of radiolabeled *Arabidopsis* seedlings, products of transport assays, and preparations of Ins(1,[^{33}P]2,3,4,5,6)P_6 were all analyzed by anion exchange HPLC on a 23.5-cm × 4.6-mm internal diameter Partisphere SAX WVS cartridge with guard cartridge (18). The column was eluted at a flow rate of 1 ml/min with a gradient derived by mixing of A, water; B, 1.25 M-$(NH_4)_2HPO_4$ adjusted to pH 3.8 with H_3PO_4 according to the following program: 0 min, 0% B; 5 min, 0% B; 65 min, 100% B; 75 min, 100% B. Radioactivity (^{3}H or ^{33}P) in column eluates was estimated by admixture of Optima Flo^{TM} AP (Canberra Packard, Pangbourne, UK) scintillation fluid at 2 ml/min in a

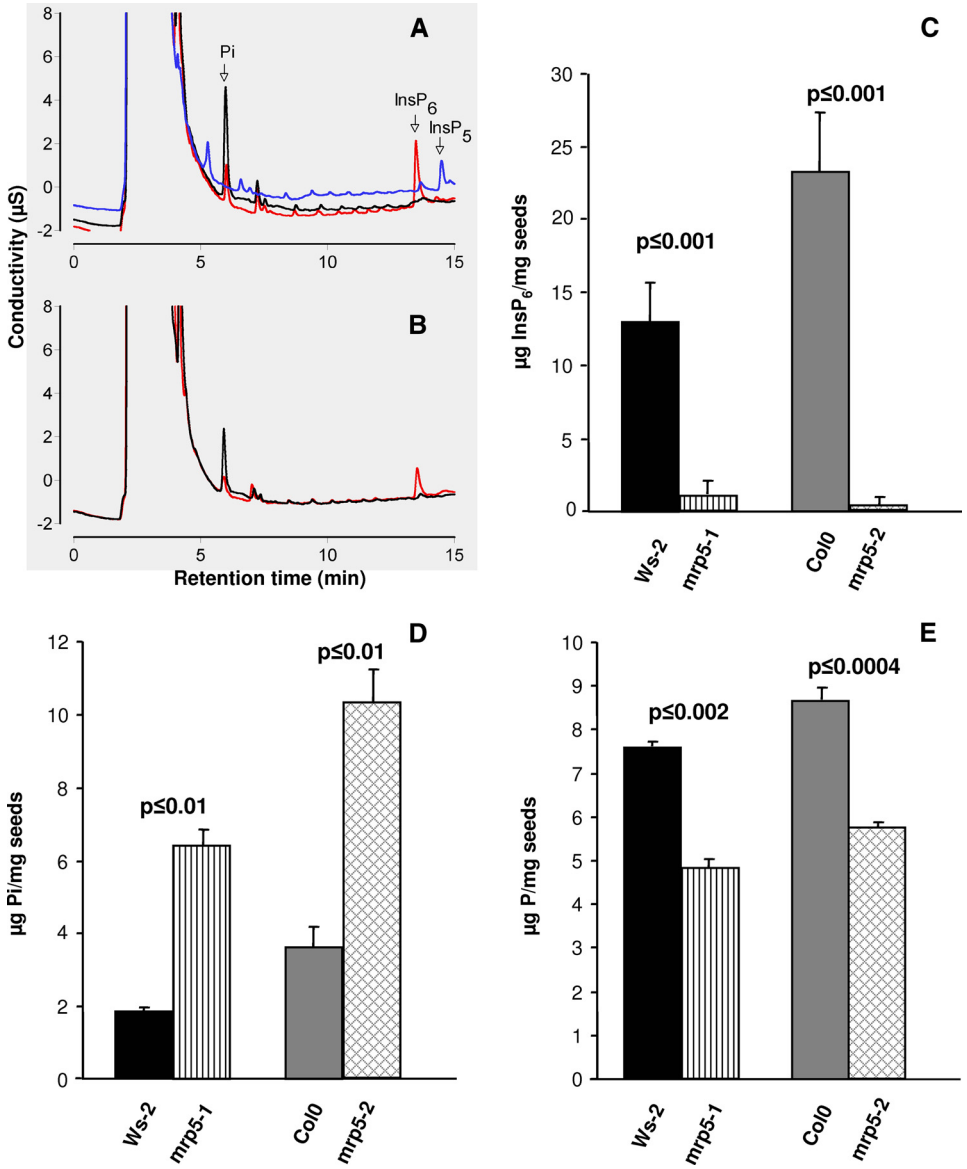

FIGURE 1. **Ablation of AtMRP5 disturbs inositol hexa*kis*phosphate, phosphate, and phosphorus levels in seeds.** The conductivity profiles of seed extracts is shown. *A*, traces for Col0 (*red line*), *mrp5-2* (*black line*), and *ipk1-1* (*blue line*). *B*, traces for Ws-2 (*red line*) and *mrp5-1* (*black line*). Individual traces are offset on the *y* axis to aid visualization. *C*, seed $InsP_6$. *D*, inorganic phosphate (*Pi*). *E*, total phosphorus (*P*) content of two independent AtMRP5 mutants and their corresponding wild types. The data represent the means and standard deviations of four to eight independent measurements.

Canberra Packard A515 flow detector fitted with a 0.5-ml flow cell. The integration interval was 0.2 min.

Analysis of Stomatal Apertures—Arabidopsis (Ws-2) leaves were transformed with the *GUS* reporter gene under control of the *MYB60* promoter (19) by particle bombardment. For detection of GUS activity, the leaves were incubated for 8 h at 37 °C in 1 mM X-glucuronic acid, 0.5% Triton X-100, 50 mM $NaHPO_4$, pH 7.2, and subsequently cleared in 70% ethanol. The *AtMRP5* cDNA under the control of the *MYB60* promoter was cloned into Gateway™ compatible plant transformation vectors (20). The resulting constructs were used to transform *mrp5-1* mutants by the floral dipping method using *Agrobacterium* (21). *Arabidopsis* plants (Ws-2, *mrp5-1*, and *MYB60::MRP5*, independent homozygous transformed lines from the T3 generation) were grown in soil in a phytotron (8-h light/16-h dark cycle; 21 °C, 70% relative humidity). For stomatal aperture measurements, the leaves of 6-week-old plants were harvested and incubated for 3 h in the light in a solution, 30 mM KCl, 1 mM $CaCl_2$, 5 mM MES-KOH, pH 5.8, with or without 5 µM ABA. Epidermal strips, prepared from the abaxial surface, were analyzed by light microscopy.

Radiolabeling of A. thaliana—Seeds of Ws-2 and *mrp5-1* were germinated and grown on a lab prepared half-strength Murashige and Skoog medium containing 2% agar. The medium was prepared to match the Duchefa (Haarlem, The Netherlands) M0221 product. The inorganic phosphate (KH_2PO_4) content of the medium was 0.625 mM. The seedlings were grown for 12 days at 22 °C under long day conditions (16-h light/8-h dark cycle) in a Sanyo (Biomedical Europe BV) MLR-351 light cabinet at a fluence rate of 120 µmol/m^2/s. The seedlings were subsequently transplanted to agar medium containing either 0.625 mM or 5 µM phosphate and grown for a further 3 days, before transfer to liquid medium with the same phosphate concentration. The seedlings were labeled in 0.5 ml of liquid medium containing 1.125 MBq *myo*-[2-^{3}H]inositol (PerkinElmer Life Sciences; specific activity, 752 GBq/mmol) in the wells of a multiwell plate for the 5-day duration of growth on liquid medium. The medium was supplemented with 0.2 ml of medium lacking radiolabel after 2 days.

RESULTS

Ablation of AtMRP5 Reduces Inositol Hexakisphosphate Level—In a recent paper it was shown for maize that the absence of an ATP-binding cassette protein, *ZmMRP4*, reduced inositol hexa*kis*phosphate accumulation in kernels (15). Phylogenetic studies of ZmMRP4 revealed that AtMRP5 is a very close homologue. Because *AtMRP5* is strongly expressed in seeds, we were interested whether knock-out mutants of this ABC transporter exhibit the same low inositol hexa*kis*phosphate phenotype. To this end, we used two independent T-DNA insertion mutants of *AtMRP5* in their different genetic backgrounds to determine their corresponding inositol hexa*kis*phosphate contents. Inositol hexa*kis*phosphate accumulates as mixed salts of mineral cations in the globoids of specialized vacuoles in *Arabidopsis* (22) as in other seeds (23).

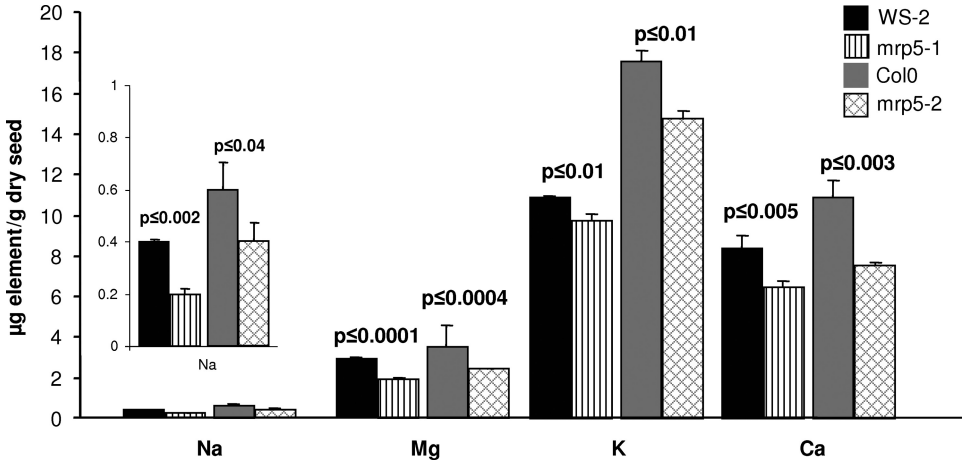

FIGURE 2. **Analysis of cation reserves in seeds of *Arabidopsis*.** Seed content of cations that differ significantly in the two independent AtMRP5 mutants (*mrp5-1* and *mrp5-2*) as compared with their corresponding wild types. The data represent the means and standard deviations of four independent measurements. *Na*, sodium; *Mg*, magnesium; *K*, potassium; *Ca*, calcium.

Seed inositol hexa*kis*phosphate was measured by suppressed ion conductivity (16, 24). Example profiles are shown in Fig. 1*A*, (note that the identity of the inositol hexa*kis*phosphate peak was confirmed for all genotypes by spiking extracts from these genotypes with an inositol hexa*kis*phosphate standard). Fig. 1*A* includes a profile of the biosynthetic mutant *ipk1-1*. On the Dionex AS11 column used, inositol 1,3,4,5,6-penta*kis* phosphate and inositol 3,4,5,6-tetra*kis*phosphate, both of which accumulate in *ipk1-1* elute after inositol hexa*kis*phosphate (24). Our analysis showed that *mrp5-1* and *mrp5-2* mutants do not accumulate inositol hexa*kis*phosphate in the seed; nor do they accumulate lower inositol phosphates, in contrast to *ipk1-1*, which accumulates inositol 1,3,4,5,6-penta*kis*phosphate and inositol 3,4,5,6-tetra*kis*phosphate predominantly among tetra*kis*phosphate species (25). Our measurements of seed inositol hexa*kis*phosphate in the Col0 genetic background of *mrp5-2*, 24.8 ± 4.1 nmol/mg of dry weight, agrees favorably with the data in Ref. 25 (22.3 ± 0.4 nmol/mg). Seed inositol hexa*kis*phosphate was reduced to 0.3 ± 0.6 nmol/mg in the *mrp5-2* mutant (Fig. 1*C*). This value and that of the *mrp5-1* mutant (1.1 ± 1.1 nmol/mg) as compared with its Ws-2 parent (14 ± 3.1 nmol/mg) are significantly greater depletions than that reported for the biosynthesis mutant *ipk1-1*, 3.9 ± 0.4 nmol/mg (25), for which we obtained a value of 4.1 ± 2.9 nmol/mg (data not shown). These data provide genetic evidence that AtMRP5 is required to accumulate inositol hexa*kis*phosphate in seeds. Measurement of inorganic phosphate levels in *mrp5* mutants and their parents (Fig. 1, *A*, *B*, and *D*) revealed that depletions of inositol phosphates in the mutants are accompanied by accumulation of inorganic phosphate. The values obtained for seeds of Col0 (35.9 ± 5.4 nmol/mg of dry weight), *mrp5-2* (103.9 ± 9.4 nmol/mg), Ws-2 (18.5 ± 1.0 nmol/mg), and *mrp5-1* (65.0 ± 4.3 nmol/mg), when compared with *atipk1-1* (30.2 ± 1.2 nmol/mg), indicate that inositol hexa*kis*phosphate transporter mutants show a seed inorganic phosphate accumulation phenotype that is more severe than that of the biosynthetic mutant *atipk1*. The measurements of total phosphorus (Fig. 1*E*) revealed a reduction, relative to wild type, respectively, of 37% in the *mrp5-1* mutant and of 34% in *mrp5-2*. We also attempted to measure inositol hexa*kis*phosphate levels in leaf tissue of *Arabidopsis*. In our hands, the levels were below the level of detection by suppressed ion conductivity, a consequence in part of a number of unidentified anions eluting in the region of inositol hexa*kis*phosphate.

It has already been extensively reported that *mrp5* mutants have pronounced phenotypes, some of which manifest in guard cells (7, 8, 26). Determinations of cations (Fig. 2) that form chelates with inositol hexa*kis*phosphate (phytin) revealed concurrent reductions in mineral composition of seeds of *mrp5-1* and *mrp5-2*. Those minerals that differed significantly between wild type parent and mutant included sodium, which was present only in very low amounts and which was reduced by 41 and 32%. Magnesium was reduced by 34 and 31%, whereas calcium was reduced by 23 and 31%. A small reduction was observed for potassium (17%), whereas no significant reduction was determined for iron, manganese, zinc, nickel, and copper. It is known that several divalent cations strongly bind to phytate, but the species can differ from plant to plant. Our data suggest that iron is not associated with phytate in *Arabidopsis*. Additional data for other minerals that were not found to differ significantly between mutant and wild type genotypes is provided in supplemental Fig. S1.

AtMRP5 Encodes a High Affinity Inositol Hexakisphosphate Transporter—The absence of lower inositol phosphates in the conductivity profiles (Fig. 1, *A* and *B*) contrasts with the biosynthetic mutant *ipk1-1* and with biosynthetic mutants, for example, of barley (27, 28) and maize (29, 30). To test whether AtMRP5 is an inositol hexa*kis*phosphate transporter or a membrane protein participating, but not directly catalyzing inositol hexa*kis*phosphate transport, we expressed AtMRP5 in yeast deficient in the YCF1 ABC transporter. Preliminary transport experiments with different mutants of MRP-type ABC transporters revealed that *ycf1* exhibited only 10–20% of the MgATP-dependent transport activity compared with the corresponding wild type strain (W303). This residual activity might be due to one of the MRP-like genes still present in *ycf1*. We were unsuccessful in our attempts to transform AtMRP5 into double and triple MRP knock-out mutants, so we used AtMRP5-transformed *ycf1* for further analysis. Microsomes were prepared and used to perform studies of [^{33}P]inositol hexa*kis*phosphate uptake. Inositol hexa*kis*phosphate transport was dependent on *AtMRP5* and ATP and was linear with respect to time up to 5.5 min (Fig. 3*A*). In the absence of AtMRP5, a low level of ATP-dependent inositol hexa*kis*phosphate uptake was observed. Expression of AtMRP5 induced a slight increase in inositol hexa*kis*phosphate transport in the absence of ATP, whereas the addition of ATP, to microsomes isolated from AtMRP5-transformed *ycf1* cells, resulted in a 6-fold increase of the ATP-dependent transport activity.

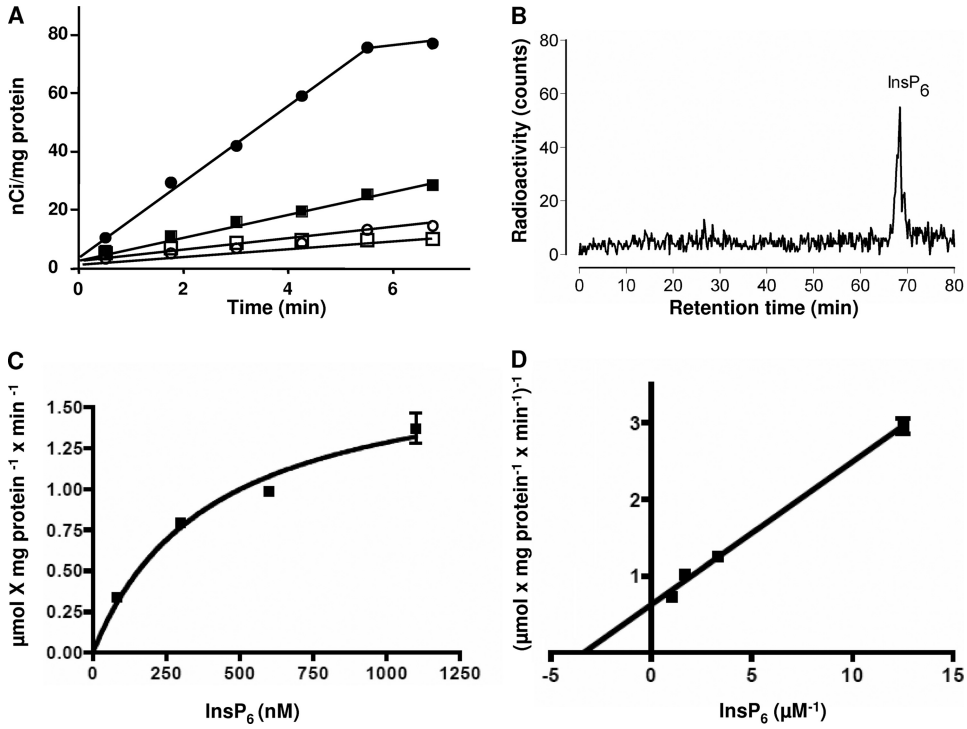

FIGURE 3. **AtMRP5 is a high affinity inositol hexa*kis*phosphate transporter.** *A*, inositol hexa*kis*phosphate uptake into microsomes isolated from yeast *ycf1* mutant cells transformed with an empty vector (pNEV) or with vector harboring *AtMRP5* cDNA (pNEV-MRP5). For non-ATP-dependent uptake, the reaction mix lacked ATP. Transport under all conditions was performed with the same vesicle preparation. *Open square*, pNEV-ATP; *filled square*, pNEV+ATP; *open circle*, pNEV-AtMRP5-ATP; *filled circles*, pNEV-AtMRP5+ATP. The $InsP_6$ concentration used for the time-dependent uptake was 80 nM. *B*, partisphere SAX HPLC analysis of the ^{33}P recovered from filtered and washed microsomes showing the integrity of inositol hexa*kis*phosphate after transport. *C*, inositol hexa*kis*phosphate uptake by microsomes isolated from yeast cells harboring AtMRP5. Uptake velocities were measured at different inositol hexa*kis*phosphate concentrations, as indicated. *D*, a double reciprocal plot was used to determine the K_m value of AtMRP5.

TABLE 1

The effect of ABC transport inhibitors on AtMRP5-mediated inositol hexa*kis*phosphate transport

Yeast microsomes were incubated in the reaction mix with the potential inhibitors at room temperature. After 8 min inositol hexa*kis*phosphate was added to the reaction mix. For the experiments with the nonhydrolyzable ATP analogue (AMPPNP), the 4 mM ATP from the reaction mix was replaced with the equivalent concentration of AMPPNP. For the experiments on ice, tubes containing the reaction mix and the labeled $InsP_6$ were placed on ice immediately after the addition of the yeast microsomes. The $InsP_6$ uptake was terminated by transfer of three aliquots onto 0.45-μm diameter pore size nitrocellulose filters after 5.5 min. The values are corrected for corresponding controls with vesicles isolated from ycf1 yeasts transformed with the empty pNEV vector. The different inhibitors and competitors were always tested using the same vesicle preparation. The reaction mix contained labeled $InsP_6$ at 1.85 kBq/nitrocellulose filter.

Condition	Percentage	Repetitions
+ ATP	100	6
+ AMPPNP	0	2
+ 5 mM NH_4Cl	77.6 ± 15.5	3
+ 150 μM glibenclamide	28.8 ± 17.8	3
+ 1 mM vanadate	62 ± 11.2	3
+ 1 mM probenicide	−12.5 ± 22.9	3
Ice	7.3 ± 7.9	2

Replacement of ATP by the nonhydrolyzable ATP analogue AMPPNP abolished transport (Table 1). This result further confirms that transport of inositol hexa*kis*phosphate is strictly ATP-dependent.

HPLC analysis of the ^{33}P recovered from filtered and washed microsomes revealed that, within the timeframe of our uptake experiments, there was no discernible metabolism of $Ins(1,[^{33}P]2,3,4,5,6)P_6$ to lower inositol phosphate species, nor to inorganic phosphate (Fig. 3*B*). Thus, the phosphate in the 2-position of inositol hexa*kis*phosphate, and the whole molecule, was metabolically stable. We did not observe phosphorylation of inositol hexa*kis*phosphate, as catalyzed by the KCS1 (31) or VIP1 (32) proteins of *Saccharomyces cerevisiae*. Inclusion of a range of ABC transport inhibitors revealed that the sufonylureas glibenclamide and probenicid had a very strong inhibitory effect on AtMRP5-mediated inositol hexa*kis*phosphate uptake (Table 1). Vanadate, which is an efficient inhibitor for most ABC-type protein-mediated transport processes, had only a partial inhibitory effect. NH_4Cl, which abolishes pH gradients had a very minor inhibitory effect, confirming that the ΔpH plays no or only a minor role in ABC transporter-mediated processes.

Transport experiments performed on ice showed that transport was abolished under these conditions, discounting the possibility that the transport activity reflected binding of inositol hexa*kis*phosphate only, or that transport was a facet of nonspecific permeability of yeast microsomes. A kinetic analysis of inositol hexa*kis*phosphate uptake was undertaken at room temperature. Uptake followed saturation kinetics. A double reciprocal plot of uptake against inositol hexa*kis*phosphate concentration yielded a linear relationship and estimations of K_m of 310 nM in one experiment and 263 nM in another (Fig. 3*C* and supplemental Fig. S2). V_{max} values reflecting the expression level of AtMRP5 were estimated at 1.6–2.5 μmol min^{-1} mg^{-1} microsome protein (Fig. 3*C*). The ATP-dependent inositol hexa*kis*phosphate transport activity from nontransformed yeast microsomes corresponded only to 10–20% of that observed with AtMRP5 expressing yeast. Therefore, the obtained K_m values should reflect closely the characteristics of AtMRP5-mediated transport.

To characterize the substrate specificity of AtMRP5, we performed competition experiments with a range of inositol polyphosphates identified in plants (Table 2). At a concentration corresponding to a 2-fold K_m of inositol hexa*kis*phosphate (600 nM), no significant inhibition was observed for $Ins(1,4,5)P_3$, $Ins(1,3,4,6)P_4$, and $Ins(1,4,5,6)P_4$. With $Ins(1,3,4,5,6)P_5$, transport was reduced by 20%. *Scyllo*-inositol hexa*kis*phosphate did not inhibit transport at 600 nM, suggesting that substrate binding exhibits stereospecificity and is not exclusively a consequence of high density of negative charge on the substrate. Estradiol glucuronide, a com-

TABLE 2

The effect of inositol polyphosphates on AtMRP5-mediated inositol hexa*kis*phosphate transport

The putative inhibitors and/or competitors were added to the reaction mix consisting of transport buffer, 1 mM dithiothreitol, 5 mM ATP, 10 mM $MgCl_2$, 10 mM creatine-phosphate, and 100 μg/ml creatine kinase at the concentration indicated above. Yeast microsomes were added to start the transport assay. The assays were performed at room temperature. After 5.5 min, inositol hexa*kis*phosphate uptake was terminated by the transfer of three aliquots/repetition onto 0.45-μm-diameter pore size nitrocellulose filters. The putative inhibitors and/or competitors were always tested using the same vesicle preparation. ATP-dependent AtMRP5-mediated transport was considered as 100%. The reaction mix contained labeled inositol hexa*kis*phosphate at 1.85 kBq/nitrocellulose filter.

Condition	Percentage	Repetitions
+ ATP	100	6
+ 600 nM		
Ins(1,4,5)P_3	111.7 ± 17.6	3
Ins(1,3,4,6)P_4	104.1 ± 18.4	3
Ins(1,4,5,6)P_4	100.6 ± 16.8	3
Ins(1,3,4,5,6)P_5	80.5 ± 6.6	2
Scyllo InsP_6	119.8 ± 12.5	3
Ins(1,2,3,4,5,6)P_6	52.7 ± 1.8	2
Estradiol glucuronide	122.6 ± 16.2	3
+1200 nM		
Ins(3,4,6)P_3	157.3 ± 3.8	3
Ins(1,3,4,6)P_4	100.8 ± 30.3	2
Ins(1,4,5,6)P_4	80.2 ± 20.2	3
Ins(1,3,4,5,6)P_5	61.0 ± 7.1	2
Scyllo InsP_6	57.7 ± 13.6	2
Ins(1,2,3,4,5,6)P_6	0 ± 0	2
Estradiol glucuronide	92.4 ± 4.9	3

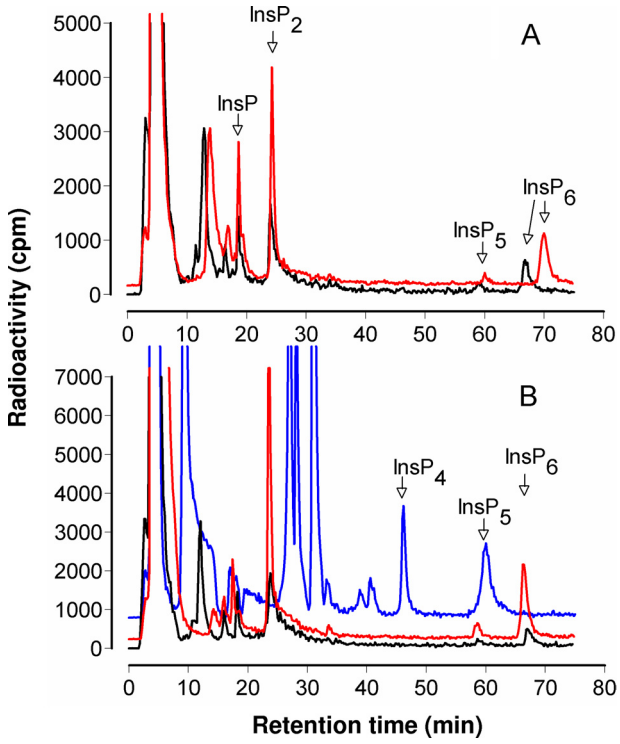

FIGURE 4. **Profiles of inositol phosphates from [^{3}H]inositol-labeled seedlings.** *A*, traces for Ws-2 labeled with low phosphate (*black line*) and high phosphate (*red line*). *B*, traces for *mrp5-1* labeled with low phosphate (*black line*) and high phosphate (*red line*) and for *ipk1-1* labeled with high phosphate (*blue line*). Note that the retention time of inositol phosphates can vary; InsP_6 was confirmed for all genotypes by spiking parallel samples with an InsP_6 standard. The *traces* for *mrp5-1* and Ws-2 labeled with high phosphate and the *ipk1-1* trace have been offset on the *y* axis to aid visualization.

pound shown to be transported by AtMRP5 (26), had a slight stimulatory effect. Increasing the concentration of the inhibitors to 1200 nM resulted in an ~40% inhibition of *myo*-inositol hexa*kis*phosphate uptake by both Ins(1,3,4,5,6)P_5 and *scyllo*-inositol hexa*kis*phosphate. Interestingly, at this concentration Ins(1,4,5)P_3 exhibited a stimulatory effect of about 50%. From this result it is tempting to speculate that Ins(1,4,5)P_3 at a higher concentration can accelerate the depletion of the cytosolic InsP_6 and thus the termination of the InsP_6 signaling pathway. In summary, these data ascribe novel function to AtMRP5, that of a specific high affinity *myo*-inositol hexa*kis*phosphate transporter.

The Inositol Phosphate Metabolism of atmrp5 Mutants Is Sensitive to External Phosphate—In the context of reduced vacuolar deposition of inositol hexa*kis*phosphate and accumulation of inorganic phosphate, the *atmrp5* transporter mutants potentially afford the opportunity to assess the interplay, previously untested, of intracellular inositol phosphate transport and inositol phosphate metabolism. Inositol hexa*kis*phosphate synthesis is responsive to phosphate supply in suspension culture of *Arabidopsis* (33). We labeled Ws-2 and *mrp5-1* seedlings with inositol and analyzed the responsiveness of inositol hexa*kis*phosphate synthesis to phosphate concentration in the growth and labeling media. Our analysis (Fig. 4) revealed that the profile of ^{3}H-labeled peaks of increasing phosphorylation, from inositol up to inositol hexa*kis*phosphate, were similar for Ws-2 and *mrp5-1* mutants treated and labeled in low phosphate. The absence of major peaks of label in the inositol 1,4,5-trisphosphate to 1,3,4,5,6-penta*kis*phosphate region is typical of plant tissues. Material eluting before the InsP peak includes inositol and, likely, cell wall sugars derived from inositol. In a typical experiment, at 5 μM phosphate, the label recovered in inositol penta*kis*phosphate and inositol hexa*kis*phosphate peaks were, respectively, 0.25 and 0.96% for Ws-2 and 0.07 and 0.60% for *mrp5-1*. These results and the seed inositol phosphate data (Fig. 1) suggest that the control exerted by AtMRP5 on inositol hexa*kis*phosphate accumulation in seeds or whole seedlings is not manifest as an accumulation of metabolic precursors. Moreover, seedlings of Ws-2 and *mrp5-1* grown and labeled on high phosphate accumulated ~2-fold more label in inositol hexa*kis*phosphate than those transferred to and labeled in low phosphate media. Similar conclusions have been drawn from measurements of inositol hexa*kis*phosphate in suspension cultures of *Catharantheus roseus* and *Arabidopsis* grown in low and high phosphate, with *Arabidopsis* showing weaker responses to phosphate than *C. roseus* (33). In our experiments, the proportions of label recovered in inositol penta*kis*phosphate and inositol hexa*kis*phosphate were 0.15 and 1.89% for Ws-2 and 0.25% and 1.46% for *mrp5-1* grown and labeled on high phosphate. These data show that, in respect to metabolic flux from inositol to inositol hexa*kis*phosphate, the *mrp5-1* mutant is responsive to environmental phosphate status like its wild type Ws-2 parent. We conclude that, unlike the *ipk1-1* mutant, which is deficient in recognition of external phosphate (25), *mrp5* mutants are not defective in sensing environmental phosphate. The data presented above indicate that AtMRP5 makes a dominant contribution to accumulation of inositol hexa*kis*phosphate in seeds of *Arabidopsis*. Although we are not aware of gene expression studies of inositol hexa*kis*phosphate accumulation in *Arabidopsis*, of the biosynthetic gene prod-

ucts, IPK1 has a dominant contribution to inositol hexa*kis*phosphate accumulation (25). We undertook expression analysis of the effect of mutation of AtMRP5 on transcript levels of AtIPK1 and of four members of the inositol tris/tetra*kis*phosphate kinase family whose contribution to inositol hexa*kis*phosphate synthesis, while undefined in *Arabidopsis* (34), is anticipated from studies of maize (30). The data presented in the supplementary information (supplemental Fig. S3) indicate that mutation of *AtMRP5* was without effect on *IPK1* or *ITPK1* (At5G16760) in either background, whereas a doubling of the other transcripts was evident in *mrp5-1* only.

Atmrp5 Mutants Show Defective Stomatal Responses That Are Partially Relieved by Guard Cell-targeted Expression of AtMRP5—The foregoing data point not only to a novel inositol hexa*kis*phosphate transport function for AtMRP5 but also to a dominant contribution to inositol hexa*kis*phosphate accumulation. ABC transport proteins have not been extensively characterized in plants, but among them AtMRP5 and AtABCB14 have been shown to exert control over a number of cellular targets, particularly ion channels whose regulation underlies the control of stomatal function. Because we have shown that inositol hexa*kis*phosphate is a physiological regulator of vacuolar (Ca^{2+}-permeable) and plasma membrane (inward rectifying K^+) conductances (13, 14), we sought to determine a role for AtMRP5 in guard cell function. We tested the effectiveness of ABA as an inhibitor of stomatal opening in response to light, because this response is a well documented physiological indicator of MRP5 function, one to which anion channel activity contributes markedly. The data of Fig. 5*C* were obtained from epidermal peels of wild type (Ws-2), the *mrp5-1* mutant, and a series of lines of *mrp5-1* that had been independently transformed with an *AtMRP5* construct driven from a promoter, MYB60, that is strongly expressed in guard cells but not in epidermal cells (Fig. 5, *A* and *B*). Stomatal opening was strongly inhibited by ABA in Ws-2 but not in the *mrp5-1* mutant (Fig. 5*C*). Significantly, transgenic expression of AtMRP5 restored ABA responsiveness to the *mrp5-1* mutant, a result that was confirmed for several independent transgenic lines. Detailed physiological analyses of the above mentioned transgenic lines revealed that guard cell-targeted expression of AtMRP5 did not restore wild type seed $InsP_6$ content (Fig. 5*D*) and did not restore the root phenotype (supplemental Fig. S4).

It remains a matter of debate whether the observed stomatal phenotype of *mrp5-1* is the result of an interaction between AtMRP5 and unknown proteins and/or the AtMRP5-mediated transport of a specific molecule. Therefore, to get further insights as to whether a functional transporter is required, site-directed mutagenesis of AtMRP5 was undertaken, and the mutated cDNAs driven by the CaMV35S promoter were transformed into *mrp5-1* (supplemental Fig. S5*A*). The *mrp5-1* related phenotypes (seed $InsP_6$ content, root length, drought resistance, and stomatal aperture) were analyzed for all constructs in the T3 generation. Most of mutants showed an intermediate phenotype as compared with Ws-2 and *mrp5-1* for all traits. Only those plants with either a D771A or a D1429A exchange in the Walker B domain of NBD1 or NBD2 behaved like *mrp5-1* (supplemental Fig. S5, *b–e*). Because the Walker B

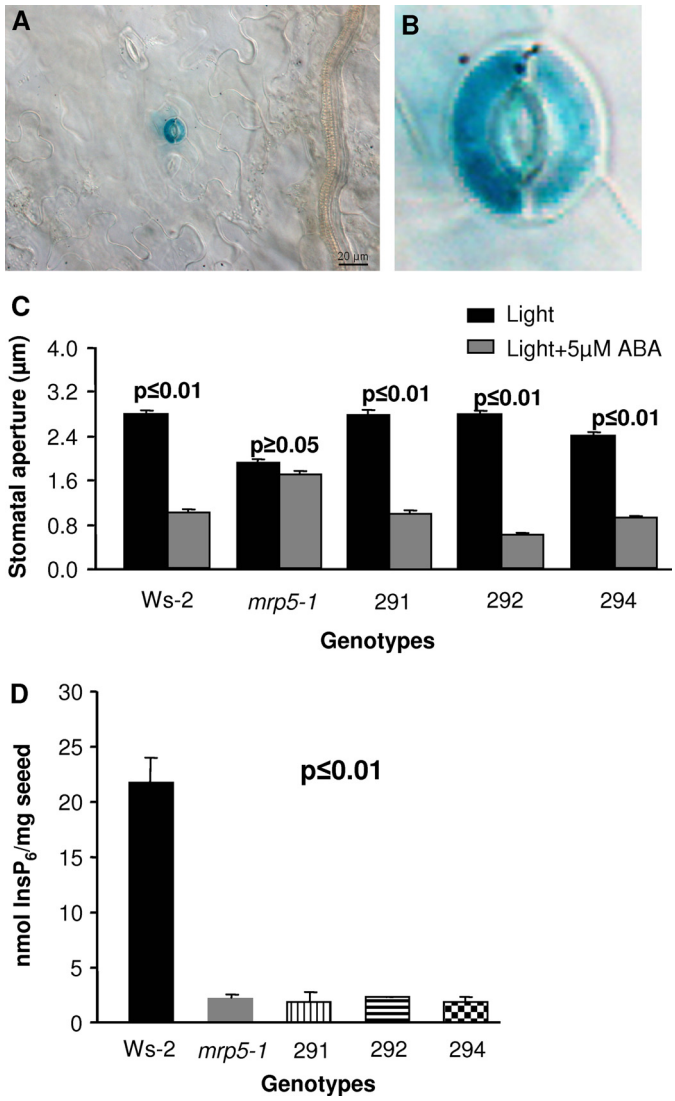

FIGURE 5. **Guard cell-targeted expression of AtMRP5 restores stomatal phenotype in AtMRP5 mutant.** *A* and *B*, the MYB60 promoter targets *GUS* exclusively to guard cells. *C*, the *mrp5-1* mutant is insensitive to ABA (ABA inhibits opening of stomata in response to light). The *MYB60::AtMRP5* transgene restores ABA sensitivity to *mrp5-1*. The results for Ws-2, *mrp5-1*, and three independent transgenic T3 lines are shown. At least 200 stomates of abaxial epidermal strips were measured for each genotype. Two independent experiments were performed, and three additional T3 lines of the transgenic gave the same results (data not shown). The *error bars* represent the S.E. *D*, the *MYB60::AtMRP5* transgene does not complement the seed inositol hexa*kis*phosphate content of *mrp5-1*. The data represent the means and standard deviations of three independent measurements. For *C*, the *p* value indicates the confidence of significance between light treatment and light+ABA treatment within the same genotype. For *D*, the *p* value indicates the confidence of significance between wild type and the four other genotypes.

domain is known to be essential for the transport activity of most ABC transporters (35), this result suggests that AtMRP5-mediated $InsP_6$ uptake and the stomatal phenotype are both dependent on a functional AtMRP5.

DISCUSSION

Inositol polyphosphates and inositol pyrophosphates contribute to diverse cell biological and developmental phenomena including activated exocytosis (36), mRNA export (37, 38), cell cycle activities (39), and establishment of left-right asymmetry

of organ development in zebra fish (40). In plants, inositol hexa*kis*phosphate mobilizes calcium and inhibits the inward rectifying K^+ conductance of guard cells (13, 14).

Despite all of these elaborations of higher inositol polyphosphate function, remarkably little is known of the compartmentation of inositol polyphosphate synthesis or of the contribution of compartmentation to the roles identified above. Interestingly, inositol hexa*kis*phosphate is a component of basal resistance to fungal, bacterial, and viral pathogens in *Arabidopsis*, with an indication that a discrete subcellular pool of inositol hexa*kis*phosphate contributes to these phenomena (41). In higher plants, inositol hexa*kis*phosphate accumulates as mixed salts of alkali and other metal cations in the globoids of specialized vacuoles of storage tissues (23). By corollary, inositol hexa*kis*phosphate is a major component of the laminal layer of hydatid cysts, the reproductive stage of the animal parasite *Echinococcus granulosus* (24). Both of these examples imply vectorial transport of inositol hexa*kis*phosphate or a precursor across cellular membranes, noncytosolic synthesis of inositol hexa*kis*phosphate, and/or trafficking of membrane-bound inositol hexa*kis*phosphate. These possibilities are all highlighted by the apparent enigma that human multiple inositol polyphosphate phosphatase localizes within the lumen of the endoplasmic reticulum, whereas its inositol phosphate substrates are considered to be exclusively cytosolic (42).

Our elaboration of AtMRP5 as an inositol hexa*kis*phosphate transporter, taken with the analysis of *ZmMRP4* mutants (15), provides a mechanistic explanation of the accumulation of inositol hexa*kis*phosphate in storage tissues of plants that differs from established conventions. Previous explanations of inositol hexa*kis*phosphate accumulation in membrane-bound protein bodies, including the aleurone bodies of cereals, are tightly linked to morphological examination of vesicle trafficking phenomena as ontogenetic explanations of the origins of protein bodies themselves (43, 44). We are reminded of analysis of natural variation of inositol hexa*kis*phosphate accumulation in *Arabidopsis*, which mapped a trait in inositol hexa*kis*phosphate accumulation to a 99-kb region that harbored a tonoplast membrane ATPase G-subunit (16). Although the exact locus of the trait was not identified, one possible explanation of the variation in inositol hexa*kis*phosphate is that accumulation of inositol hexa*kis*phosphate is dependent on vacuolar transport processes.

We now show that two distinct insertion mutants of *AtMRP5* (Col0 and Ws-2) in different, genetic backgrounds both display a low phytic acid phenotype in seed tissue. We show that the low inositol hexa*kis*phosphate seed phenotype is associated with alterations of mineral cation and phosphate status in both genetic backgrounds. The low seed phytate phenotype is a direct consequence of the missing transport activity. Our data demonstrate that AtMRP5 is a specific, high affinity inositol hexa*kis*phosphate transporter.

Beyond our identification of the molecular identity of an inositol phosphate transporter, our analysis reveals, in the context of existing literature, that disruption of a gene encoding an inositol hexa*kis*phosphate transporter contributes to stomatal biology. Because we show that MRP5 expression, exclusively, in guard cells of the *mrp5-1* mutant restores sensitivity of these cells to ABA, we hypothesize that AtMRP5 is involved in stomatal regulation because of its capacity to transport inositol hexa*kis*phosphate. The physiology of guard cells is dominated by the multitude of ion channels and transporters whose

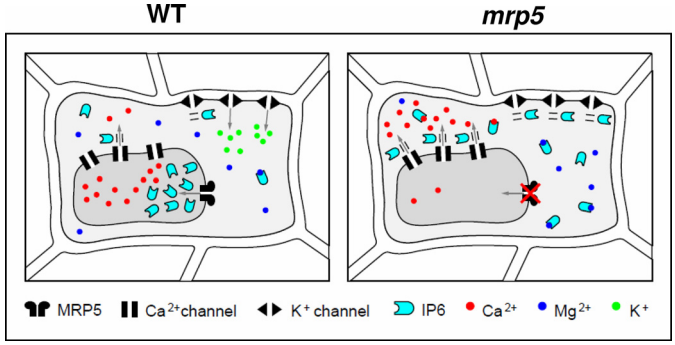

FIGURE 6. **Hypothetical model that links AtMRP5, $InsP_6$ signaling and guard cell movements.** In wild type plants, inositol hexa*kis*phosphate stimulates the release of Ca^{2+} by specific channels and inhibits the K^+ inward channel. To avoid continuous $InsP_6$ signaling, inositol hexa*kis*phosphate has to be transported into the vacuole by AtMRP5. AtMRP5 mutant plants are impaired in the export of $InsP_6$ into the vacuole. Increased concentrations of cytosolic $InsP_6$ might complex divalent cations or induce continuous Ca^{2+} release, thus disturbing Ca^{2+}-dependent signaling pathways. Furthermore, during the light period, increased $InsP_6$ levels may reduce K^+ uptake into guard cells by inhibiting K^+ inward rectifying channels.

regulation is integrated in this specialized epithelial cell, with tonoplast transport playing a central role (2). It may be significant that the fast and slow Ca^{2+}-permeable conductances of the tonoplast are both targets of inositol hexa*kis*phosphate (13). For the meantime, in the absence of direct studies of electrophysiological targets of inositol hexa*kis*phosphate in our transgenics of *mrp5-1*, it remains plausible that perturbation of cytosolic and/or vacuolar inositol hexa*kis*phosphate concentration because of the absence of its transporter will necessarily deregulate the transport processes that underlie guard cell physiology (Fig. 6).

In consideration of tonoplast function, we suggested in a first report (8) that Ca MV35S promoter-driven AtMRP5-GFP was localized to the plasma membrane of root cells. It is possible that plasma membrane localization is an ectopic consequence of MRP5 overexpression. Indeed, proteomic analysis predicts AtMRP5 to reside in the vacuolar membrane (45). The latter interpretation is consistent with the low seed inositol hexa*kis*phosphate phenotype of *mrp5-1* and *mrp5-2* mutants; $InsP_6$ is recognized to accumulate in membrane-bound protein bodies of vacuolar nature. To further address the physiological location of AtMRP5, we have examined the location of AtMRP5 expressed under the control of its native promoter. No GFP signal was detected when plants were cultivated under control conditions. Because transcriptomic studies indicated that *AtMRP5* transcript levels are increased upon drought stress (46), we subjected *mrp5-1* plants expressing AtMRP5 under the control of its native promoter to 14 days of drought stress. Under such conditions, a weak fluorescence signal associated with the vacuolar membrane was detected (supplemental Fig. S6).

These localization studies raise the intriguing question of how a vacuolar inositol hexa*kis*phosphate transporter could affect guard cell signaling and the plasma membrane anion channel activity. A hypothetical model linking the phenomena mentioned above is presented in Fig. 6. The impaired AtMRP5-dependent transport of inositol hexa*kis*phosphate into the vacuole could lead to an increase in cytosolic $InsP_6$, which could act either by complexing divalent cations such as Mg^{2+} and Ca^{2+} or triggering a continuous efflux of Ca^{2+} into the cytosol by an $InsP_6$-regulated channel. This could lead in both cases to a dis-

turbance of Ca^{2+}-dependent signaling pathways. This hypothesis could explain the impaired ABA and Ca^{2+} signaling observed in *mrp5* mutants. However, it cannot be excluded that the impaired stomatal aperture observed in the *mrp5* mutants during the light phase is not additionally the result of increased $InsP_6$ binding to unidentified targets or Ca^{2+}-dependent inhibition of the K^+ inward channel (14).

In conclusion, our identification of a high affinity inositol hexa*kis*phosphate transport associated with the tonoplast membrane adds to the diversity of functions assigned to the ABC transporter class of membrane proteins and also answers a long standing question of how inositol phosphates traverse membranes. Given the ubiquity of this class of proteins, we can anticipate that inositol phosphate transport will contribute not only to the regulation of diverse cellular signaling phenomena, perhaps to human disease, but also potentially to the acquisition of environmental inositol hexa*kis*phosphate, which comprises one of the most abundant sources of organic phosphate in the environment (47).

Acknowledgments—We are grateful to Thomas Flura (Eidgenössische Technische Hochschule, Zürich, Switzerland) for the inductively coupled plasma measurements and to Maik Hadorn for drawing the model.

REFERENCES

1. Hetherington, A. M. (2001) *Cell* **107,** 711–714
2. MacRobbie, E. A. (1998) *Philos. Trans. R. Soc. Lond. B Biol. Sci.* **353,** 1475–1488
3. Lebaudy, A., Vavasseur, A., Hosy, E., Dreyer, I., Leonhardt, N., Thibaud, J. B., Véry, A. A., Simonneau, T., and Sentenac, H. (2008) *Proc. Natl. Acad. Sci. U.S.A.* **105,** 5271–5276
4. Vahisalu, T., Kollist, H., Wang, Y. F., Nishimura, N., Chan, W. Y., Valerio, G., Lamminmäki, A., Brosché, M., Moldau, H., Desikan, R., Schroeder, J. I., and Kangasjärvi, J. (2008) *Nature* **452,** 487–491
5. Negi, J., Matsuda, O., Nagasawa, T., Oba, Y., Takahashi, H., Kawai-Yamada, M., Uchimiya, H., Hashimoto, M., and Iba, K. (2008) *Nature* **452,** 483–486
6. Lee, M., Choi, Y., Burla, B., Kim, Y. Y., Jeon, B., Maeshima, M., Yoo, J. Y., Martinoia, E., and Lee, Y. (2008) *Nat. Cell Biol.* **10,** 1217–1223
7. Klein, M., Perfus-Barbeoch, L., Frelet, A., Gaedeke, N., Reinhardt D., Mueller-Roeber, B., Martinoia, E., and Forestier, C. (2003) *Plant J.* **33,** 119–129
8. Suh, S. J., Wang, Y. F., Frelet, A., Leonhardt, N., Klein, M., Forestier, C., Mueller-Roeber, B., Cho, M. H., Martinoia, E., and Schroeder, J. I. (2007) *J. Biol. Chem.* **282,** 1916–1924
9. Schwiebert, E. M., Egan, M. E., Hwang, T. H., Fulmer, S. B., Allen, S. S., and Cutting, G. R. (1995) *Cell* **81**, 1063–1073
10. Yang, L., Reece, J., Gabriel, S. E., and Shears, S. B. (2006) *J. Cell Sci.* **119,** 1320–1328
11. Vajanaphanich, M., Schultz, C., Rudolf, M. T., Wasserman, M., Enyedi, P., Craxton, A., Shears, S. B., Tsien, R. Y., Barrett, K. E., and Traynor-Kaplan, A. (1994) *Nature* **371,** 711–714
12. Mitchell, J., Wang, X., Zhang, G., Gentzsch, M., Nelson, D. J., and Shears, S. B. (2008) *Curr. Biol.* **18,** 1600–1605
13. Lemtiri-Chlieh, F., MacRobbie, E. A., Webb, A. A., Manison, N. F., Brownlee, C., Skepper, J. N., Chen, J., Prestwich, G. D., and Brearley, C. A. (2003) *Proc. Natl. Acad. Sci. U.S.A.* **100,** 10091–10095
14. Lemtiri-Chlieh, F., MacRobbie, E. A., and Brearley, C. A. (2000) *Proc. Natl. Acad. Sci. U.S.A.* **97,** 8687–8692
15. Shi, J., Wang, H., Schellin, K., Li, B., Faller, M., Stoop, J. M., Meeley, R. B., Ertl, D. S., Ranch, J. P., and Glassman, K. (2007) *Nat. Biotechnol.* **25,** 930–937
16. Bentsink, L., Yuan, K., Koornneef, M., and Vreugdenhil, D. (2003) *Theor. Appl. Genet.* **106,** 1234–1243
17. Tommasini, R., Evers, R., Vogt, E., Mornet, C., Zaman, G. J., Schinkel, A. H., Borst, P., and Martinoia, E. (1996) *Proc. Natl. Acad. Sci. U.S.A.* **93,** 6743–6748
18. Sweetman, D., Johnson, S., Caddick, S. E., Hanke, D. E., and Brearley, C. A. (2006) *Biochem. J.* **394,** 95–103
19. Cominelli, E., Galbiati, M., Vavasseur, A., Conti, L., Sala, T., Vuylsteke, M., Leonhardt, N., Dellaporta, S. L., and Tonelli, C. (2005) *Curr. Biol.* **15,** 1196–1200
20. Curtis, M. D., and Grossniklaus, U. (2003) *Plant Physiol.* **133,** 462–469
21. Clough, S. J., and Bent, A. F. (1998) *Plant J.* **16,** 735–743
22. Otegui, M. S., Capp, R., and Staehelin, L. A. (2002) *Plant Cell* **14,** 1311–1327
23. Lott, J. N. (1984) in *Seed Physiology* (Murray, D. R., ed) Vol. 1, pp. 139–166, Academic Press, New York
24. Casaravilla, C., Brearley, C., Soulé, S., Fontana, C., Veiga, N., Bessio, M. I., Ferreira, F., Kremer, C., and Díaz, A. (2006) *FEBS J.* **273,** 3192–3203
25. Stevenson-Paulik, J., Bastidas, R. J., Chiou, S. T., Frye, R. A., and York, J. D. (2005) *Proc. Natl. Acad. Sci. U.S.A.* **102,** 12612–12617
26. Gaedeke, N., Klein, M., Kolukisaoglu, U., Forestier, C., Müller, A., Ansorge, M., Becker, D., Mamnun, Y., Kuchler, K., Schulz, B., Mueller-Roeber, B., and Martinoia, E. (2001) *EMBO J.* **20,** 1875–1887
27. Hatzack, F., Hübel, F, Zhang, W., Hansen, P. E., and Rasmussen, S. K. (2001) *Biochem. J.* **354,** 473–480
28. Dorsch, J. A., Cook, A., Young, K. A., Anderson, J. M., Bauman, A. T., Volkmann, C. J., Murthy, P. P., and Raboy, V. (2003) *Phytochemistry* **62,** 691–706
29. Raboy, V., Gerbasi, P. F., Young, K. A., Stoneberg, S. D., Pickett, S. G., Bauman, A. T., Murthy, P. P., Sheridan, W. F., and Ertl, D. S. (2000) *Plant Physiol.* **124,** 355–368
30. Shi, J., Wang, H., Wu, Y., Hazebroek, J., Meeley, R. B., and Ertl, D. S. (2003) *Plant Physiol.* **131,** 507–515
31. Saiardi, A., Erdjument-Bromage, H., Snowman, A. M., Tempst, P., and Snyder, S. H. (1999) *Curr. Biol.* **9,** 1323–1326
32. Mulugu, S., Bai, W., Fridy, P. C., Bastidas, R. J., Otto, J. C., Dollins, D. E., Haystead, T. A., Ribeiro, A. A., and York, J. D. (2007) *Science* **316,** 106–109
33. Mitsuhashi, N., Ohnishi, M., Sekiguchi, Y., Kwon, Y. U., Chang, Y. T., Chung, S. K., Inoue, Y., Reid, R. J., Yagisawa, H., and Mimura, T. (2005) *Plant Physiol.* **138,** 1607–1614
34. Sweetman, D., Stavridou, I., Johnson, S., Green, P., Caddick, S. E., and Brearley, C. A. (2007) *FEBS Lett.* **581,** 4165–4171
35. Frelet, A., and Klein, M. (2006) *FEBS Lett.* **580,** 1064–1084
36. Illies, C., Gromada, J., Fiume, R., Leibiger, B., Yu, J., Juhl, K., Yang, S. N., Barma, D. K., Falck, J. R., Saiardi, A., Barker, C. J., and Berggren, P. O. (2007) *Science* **318,** 1299–1302
37. York, J. D., Odom, A. R., Murphy, R., Ives, E. B., and Wente, S. R. (1999) *Science* **285,** 96–100
38. Odom, A. R., Stahlberg, A., Wente, S. R., and York, J. D. (2000) *Science* **287,** 2026–2029
39. Lee, Y. S., Mulugu, S., York, J. D., and O'Shea, E. K. (2007) *Science* **316,** 109–112
40. Sarmah, B., Latimer, A. J., Appel, B., and Wente, S. R. (2005) *Dev. Cell* **9,** 133–145
41. Murphy, A. M., Otto, B., Brearley, C. A., Carr, J. P., and Hanke, D. E. (2008) *Plant J* **56,** 638–652
42. Craxton, A., Caffrey, J. J., Burkhart, W., Safrany, S. T., and Shears, S. B. (1997) *Biochem. J.* **328,** 75–81
43. Adams, C., Norby, S. W., and Rinne, R. W. (1985) *Crop Sci.* **25,** 255–262
44. Marty, F. (1997) in *Advances in Botanical Research: The Plant Vacuole* (Leigh, R. A., and Sanders, D., eds) Vol. 25, pp. 1–42, Academic Press, London
45. Jaquinod, M., Villiers, F., Kieffer-Jaquinod, S., Hugouvieux, V., Bruley, C., Garin, J., and Bourguignon, J. (2007) *Mol. Cell. Proteomics* **6,** 394–412
46. Zimmermann, P., Hirsch-Hoffmann, M., Hennig, L., and Gruissem, W. (2004) *Plant Physiol.* **136,** 2621–2632
47. Turner, B. L., Papházy, M. J., Haygarth, P. M., and McKelvie, I. D. (2002) *Philos. Trans. R. Soc. London B Biol. Sci.* **357,** 449–469